Gold Nanoparticles Induce Cell Stress by Interfering with the Cellular Protein Quality Control System

Guofang Zhang
Shenzhen Institutes of Advanced Technology
Qingle Song
Shenzhen Institutes of Advanced Technology
Yuqian Zhang
Shenzhen Institutes of Advanced Technology
Ruijing Liang
Shenzhen Institutes of Advanced Technology
Liang Chen
Shenzhen Institutes of Advanced Technology https://orcid.org/0000-0002-4875-5811
Nancy Monteiro-Riviere
Kansas State University https://orcid.org/0000-0002-0132-0861
Diana Boraschi
PRD College
Yan-Zhong Chang
Hebei Normal University
Hongchang Li
Shenzhen Institutes of Advanced Technology
Yang Li (yang.li@siat.ac.cn)
Shenzhen Institutes of Advanced Technology

Article

Keywords: Protein quality control, ER stress, ER-associated degradation, Unfolded protein response, Au NPs

Posted Date: October 15th, 2020

DOI: https://doi.org/10.21203/rs.3.rs-84361/v1

Abstract

The cellular protein quality control (PQC) system ensures the intracellular misfolded/unfolded proteins to be detected and eliminated. ER-associated degradation (ERAD) and unfolded protein response (UPR) are the key mechanisms of PQC, which maintain protein homeostasis and ensure cell survival. Here, we show that after internalization by human epithelial cells, gold (Au) nanoparticles (NPs) localized in endoplasmic reticulum (ER) and induced an accumulation of misfolded/unfolded proteins. Au NPs activated UPR, but suppressed ERAD shown by a reduced degradation rate of the ERAD marker CD3-δ-YFP, which triggered ER stress through IRE1-XBP1-Chaperones and PERK-eIF2α-ATF4-CHOP pathways. The Au NP-dependent ER stress consequently induced the intracellular accumulation of ROS, and caused cell apoptosis/death, concomitant to production/release of inflammatory cytokines and chemokines. This study for the first time shows that NPs can interfere with the cellular PQC system by impairing ERAD activity, which in turn initiates a cascade of events leading to cell death and inflammation.

Introduction

The safety of engineered nanoparticles (NPs) is one of the most extensively addressed issues in the context of nanotechnological development and applications[1,2]. Within nanosafety studies, focusing on the interaction of NPs with biological systems, the interaction with proteins has received particular attention. The function of NPs can be profoundly affected by protein coating[3], and vice-versa NPs can strongly affect protein conformation, so that they could be used to destroy proteins or protein aggregates extracellularly[4]. Despite the many studies on the capacity of NP to interact with protein in the extracellular milieu or in cell-free conditions, and despite the abundant evidence of NP internalization by cells, if and how NPs can interact with intracellular proteins is still unknown.

The correct production and folding of structural and effector proteins are crucially important for the cell life and functions. Thus, cells are endowed with the so called protein quality control (PQC) system for maintaining a healthy protein homeostasis in cells[5]. Proteins are synthesized within the endoplasmic reticulum (ER), which acts as a protein biosynthesis and modification factory. Within the newly synthesized proteins in the ER, improperly folded proteins can be produced that, if not eliminated timely, will trigger ER stress and consequently lead to cell death[6]. Hence, the PQC system is evolved and used by cells to identify and eliminate the misfolded/unfolded proteins, thereby maintain protein homeostasis and preventing ER stress[5]. The dysregulation of PQC is associated with Alzheimer's disease, cancer, as well as other diseases, and has been proved critical for human healthy[7-9].

The ER related PQC machinery encompasses two key elements, the ER-associated degradation (ERAD) and the unfolded protein response (UPR) (Schema 1)[10]. The ERAD works as the first step to detect, transfer the misfolded/unfolded proteins from ER to cytosol for their degradation through ubiquitination (Schema 1). ERAD failures, even partial, may lead to sufficient accumulation of anomalous proteins for inducing ER stress, which in turn activates the UPR as a feedback mechanism. The UPR modulates the

expression of ERAD genes in order to restore ER homeostasis and promote cell survival. The UPR is activated by three sensors: the protein kinase RNA (PKR)-like ER kinase (PERK), the activating transcription factor 6 α (ATF6α), and the inositol-requiring kinase 1 (IRE1)[11-13]. In ER homeostasis, the molecular chaperone BiP binds to and sequesters the three sensors, thereby preventing UPR activation[14]. However, in the PQC process, BiP can recognize and bind to the misfolded/unfolded proteins and contribute to their elimination by either inducing their correct folding or the cytosol transferring and subsequent degradation during the ERAD process (Schema 1)[15]. In these circumstances, BiP is engaged by the misfolded/unfolded proteins and cannot sequester the three UPR sensors, which can therefore initiate the UPR signaling for ER homeostasis recovery[14]. While modulation of ERAD and UPR has been described for many drugs and other agents[16], so far no information is available on the capacity of nanomaterials to interact and modulate the cellular PQC system.

Gold nanoparticles (Au NPs) have been extensively used in biomedical applications because of their unique physicochemical and optical properties[17]. Many studies have addressed the safety of Au NPs by examining their biocompatibility, cytotoxicity and immunotoxicity[18,19]. Because of their potential biomedical applications, it is of key importance to understand if and how Au NPs can affect human cells and induce cell death and inflammation. Knowledge of the subcellular and molecular mechanisms underlying toxic/inflammatory effects will not only shed light on some fundamental aspects of the nano-bio interactions, but it can pave the way for the successfully clinical application of Au NPs.

Some evidence is available on the interaction of Au NPs with the ER. It has been reported that the Au NPs can localize in ER and Golgi in B16F10 mouse melanoma cells[20]. Branched polyethyleneimine (BPEI)-coated Au NPs with therapeutic miRNA loading have been found to targeting ER in human mesenchymal stem cells and promote osteogenic differentiation[21]. Another report showed that the intracellular accumulation of Au NPs can cause ER stress and apoptosis in human neutrophils[22]. A proteomic study showed that cell death caused by Au NPs in human chronic myelogenous leukemia cells was associated with a strong ER stress response[23]. Although there are many publications on NP-induced ER stress, little information is available on the underlying mechanisms. The hypothesis of our study is that Au NPs may cause ER stress by inducing protein misfolding/unfolding. While there is no evidence that Au NPs can cause intracellular protein misfolding, this is suggested by their capacity to affect the folding of extracellular proteins. Deng *et al.* showed that poly (acrylic acid)-coated Au NPs can cause unfolding of plasma fibrinogen extracellularly[24]. Binding of bovine serum albumin to the surface of Au NPs can cause significant conformational changes in the protein secondary structure, resulting in less a-helix content and more open structures[25,26]. In addition, we may hypothesize that Au NPs could cause ER stress not only by inducing protein misfolding but also by promoting their accumulation, *i.e.* by interfering with the function of the intracellular PQC system.

To study the possible interference of Au NPs with the PQC system, we have chosen to study human primary epithelial cells, because these cells are the first barrier/defence line that protect the body from external agents[27]. In a stress condition, epithelial cells could synthesize and secrete many cytokines to

alarm the immune defensive system of the impending danger, and recruit immune/inflammatory cells to the affected site[27]. The vigorous protein synthesis in epithelial cells makes them a good model for PQC studies. Therefore, the objective of this study was to investigate the potential effects of Au NPs on the PQC system in human cells and the molecular mechanism of the subsequent NP-induced ER stress. Thus, we have evaluated the intracellular location of Au NPs and the NP-induced protein misfolding/unfolding. Then we have assessed the subsequent Au NPs effects on the mechanisms of ERAD and UPR, and analysed the Au NP-induced ER stress, inflammatory activation and cell death. In this context, we have evaluated the role of the protein corona of Au NPs in mediating the effects on the PQC system and eventual cell toxicity/inflammation.

Results

Characterization of Au NPs

The Au NPs that we used in this study were spherical NPs with 40 nm in diameter and functionalized with BPEI (branched polyethyleneimine). We characterized the Au NPs with transmission electron microscopy (TEM), ultraviolet-visible (UV-VIS) spectrophotometry and DLS analysis, which indicated a mean hydrodynamic diameter of 50 nm and positive surface charge (Fig. 1a-c, Table 1). The hydrodynamic diameter of Au NPs was generally larger than the core particle size observed by TEM. Formation of a protein corona on Au NPs, by incubation with human plasma, caused an increase in the hydrodynamic diameters and a negative Z-potential (Table 1). The characterization of FITC-functionalized BPEI-Au NPs was shown in Supplementary Fig. 1, which indicated a successful FITC conjugation.

Since bacterial endotoxin is a common, highly biologically active contaminant that can mask the biological effects of NPs, were screened Au NPs for endotoxin and confirmed a contamination of less than 2 EU/mg particles. This low contamination ensures that we can reliably attribute to Au NPs the biological effects assessed in this study, excluding a significant contribution by biologically active exogenous contaminants such as endotoxin[28-30]. The cytotoxicity of the Au NPs was assessed *in vitro*. Human primary epithelial cells (HEK cells) were exposed to Au NPs at various concentrations for 24 h. A significant decrease in cell viability was evident upon exposure to Au NPs, with a calculated the half maximal inhibitory concentration (IC50) as 70 μg/ml, and a 10% inhibitory concentration (IC10) as 32 μg/ml (Fig. 1d).

Uptake and intracellular location of Au NPs

To investigate the potential cytotoxicity mechanism that induced by Au NPs, we monitored the targets of Au NPs in the subcellular organelles. The uptake and intracellular localization of Au NPs were examined with ICP-MS and TEM. Cells were exposed to the Au NPs for 1 h and 24 h. TEM images indicated that Au NPs were readily internalized by cells (Fig. 2a), and the ICP-MS data showed that the uptake was time-dependent (Fig. 2b). Au NPs showed concentration at the cell membrane and in areas surrounding the nucleus (Fig. 2a). Since the ER always adheres to the outer membrane of nucleus, we have examined the

possible co-localization of the internalized Au NPs with ER. In addition to TEM ultrastructural observation showing a co-localization (Fig. 2c), we could observe by confocal microscopy that a part of the FITC-labelled Au NPs co-localized with ER, as shown by the yellow fluorescence due to overlap of the green fluorescence (Au NPs) with red fluorescence (ER) in Figure 2d. The confocal fluorescent signal analysis (Fig. 2e) confirmed the co-localization of Au NPs and ER in cells (green and red peak overlap). Therefore, our results in Figure 2 suggested that the Au NPs were internalized in cells, and a part of these internalized Au NPs could translocate to the ER.

Au NPs promote the intracellular accumulation of the misfolded protein

The association of Au NPs with the ER made us think that these Au NPs may interfere with the ER functions and possibly cause the accumulation of misfolded/unfolded proteins. We thus assessed the level of the intracellular misfolded/unfolded proteins marker, Lys48-linked polyubiquitin (K48 polyUb)[31], in cells exposed to Au NPs. The result in Fig. 3a showed that K48 polyUb conjugates were significantly increased in the insoluble pellet (P) of cells treated with Au NPs, but not in the soluble supernatant (SN), when compared with untreated control cells. Since misfolded/unfolded proteins are always in the insoluble pellet[32], our result suggests that the treatment with Au NPs could increase the intracellular levels of misfolded/unfolded proteins, which would enhance the PQC process. To assess the PQC activation, we have measured the upregulation of some important PQC genes, *i.e.*, those encoding the chaperones HSP70, HSP90 (in the cytoplasm) and BiP (in the ER), which are responsible for identification and re-shaping of unfolded/misfolded proteins to their native and functional conformation[14]. Data in the Fig. 3b show that expression of *BIP*, *HSP70* and *HSP90* genes was significantly increased in cells exposed to Au NPs at 75 µg/ml. The expression results were confirmed by the analysis of the intracellular levels of the proteins HSP70, HSP90 and BiP (Fig. 3c), which showed a significant increase of BiP and a less pronounced increase of HSP70 and HSP90. These results suggest the activation/enhancement of the PQC process in response to cell treatment with Au NPs.

Au NPs interfere with the ERAD function

The PQC process occurs in the ER, whose fundamental functions are maintaining correct protein biosynthesis and modifications[33]. Having shown that Au NPs can localize in the ER, induce the accumulation of misfolded/unfolded proteins and thereby enhance the PQC process, we asked whether Au NPs could also interfere with ER functions and induce ER stress. To this end, we have investigated the effect of cell exposures to Au NPs on ERAD, the PQC process responsible for misfolded/unfolded proteins clearance in ER.

To assess the ERAD function, we have investigated the stability of the protein CD3-δ, a subunit of the T cell receptor that is a well-established ERAD substrate, and whose accumulation indicates ERAD dysfunction/inhibition[34,35]. We have transfected our cells with CD3-δ linked to the fluorescent protein YFP, and examined its degradation (in the presence of cycloheximide -CHX- to inhibit new protein synthesis) upon cell exposure to Au NPs. Results in the Fig. 3d and e show that the degradation rate of the CD3-δ-

YFP protein was greatly inhibited in NP-treated cells, resulting in its accumulation, compared to control cells. This implies that treatment with Au NPs reduces ERAD and impairs ER functions, a fact that would lead to the intracellular accumulation of misfolded/unfolded proteins.

As already mentioned, BiP is a chaperone engaged in correcting misfolded/unfolded proteins to their native and functional conformation. We can hypothesize an upregulation of BiP in cells exposed to Au NPs as consequence of the accumulation of misfolded/unfolded proteins (Fig. 3c). To further elucidate the ERAD reduction in Au NP-treated cells, we have evaluated the stability of the BiP protein, again by assessing the protein level at different times after the block of new protein synthesis with CHX. While stable in the control group, the BiP protein was significantly decreased in Au NP-treated cells (Fig. 3d and e). Further, BiP could steadily expressed in thapsigargin (TG) treated cells (Supplementary Fig. 2a-c). This implies that, although BiP expression is upregulated in Au NP-treated cells, the BiP protein is unstable and not enough thereby hampering its functions. Thus, the accelerated degradation of BiP in Au NP-treated cells can ultimately induce the further accumulation of misfolded/unfolded proteins in cells. These results suggest ERAD dysfunction and impaired PQC capacity in cells treated with Au NPs, leading to accumulation of misfolded/unfolded proteins that cannot be eliminated timely. This would ultimately induce ER stress and consequent cell death.

Au NPs effects on UPR and ER stress

The unfolded protein response (UPR) is the mechanism activated in cells to alleviate the ER stress conditions caused by accumulation of misfolded/unfolded proteins, and re-establish ER homeostasis[36, 37]. UPR failures lead to ER stress and consequent cell stress and eventual apoptosis[38,39]. The gene expression of the UPR signalling pathways initiated by the three sensors PERK, ATF6α and IRE1, those involved in ER stress were screened by a specific PCR array. As shown in the Figure 4a, no significant variation was observed in *ATF6* expression in cells exposed to Au NPs, while the PERK and IRE1 downstream genes, *ATF4, CHOP, ERO1A, ERO1B* and *XBP1* were upregulated.

To better examine the participation of the three UPR pathways in the Au NPs effects, qPCR and WB were used to verify the results of PCR array. We confirmed that ATF6 mRNA expression and protein synthesis was not increased in cells exposed to Au NPs (Supplementary Fig. 3a and b), suggesting that the ATF6 pathway is not activated in response to Au NP treatment. The activation of both the IRE1 and PERK signaling pathways was confirmed (Fig. 4b-c and Supplementary Fig. 3c). In UPR activation, the ER stress-activated endonuclease IRE1 splices the *XBP1* mRNA to *sXBP1* (spliced XBP1), which encodes the functional sXBP1, a transcriptional factor that induces the expression of ERAD genes that contribute to elimination of misfolded proteins. On the other hand, the unspliced *XBP1* mRNA (*usXBP1*) produces an antagonist of sXBP1[40]. The mRNA expression of *IRE1B*, *sXBP1* and *usXBP1* was assessed and found upregulated in cells exposed to Au NPs (Fig. 4b). It should be noted that the *usXBP1* mRNA was significantly upregulated by treatment with 25 mg/ml of Au NPs, while the mRNA of sXBP1 was not. This would shift the balance between the functional transcription factor (sXBP1) and its inhibitor (usXBP1) towards inhibition of transcription of the XBP1 target genes, including *HERPUD1*. Indeed, data in the Fig.

4d show that ERAD-related genes (*HERPUD1* and *UBQLN2*) are upregulated in cells treated with of Au NPs at the high concentration (75 mg/ml) but downregulated at the lower concentration (25 mg/ml). HERPUD1 facilitates the ERAD process by acting as a shuttle factor to deliver ubiquitination substrates to the proteasome for degradation[41], and the UBQLN2 protein participates in the ubiquitin degradation process of the ERAD. The levels of PERK and its downstream p-eIF2α, eIF2α, ATF4 and CHOP proteins were all expressed at higher levels in cells treated with Au NPs (Fig. 4c). CHOP, the final protein in the PERK signaling pathway (PERK-eIF2α-ATF4-CHOP), leads to the ER stress-induced apoptosis and is often used as an evidence of ER stress. We also observed an increase, in cells exposed to Au NPs, of the ER stress genes ER oxidoreductase 1A (*ERO1A*) and *ERO1B* (Fig. 4e and Supplementary Fig. 3d). All these results suggest that the exposure to Au NPs induces a PQC dysfunction in the ER, leading to ER stress, most likely through the PERK and IRE1 pathways.

Au NPs cause ER-dependent cell stress and inflammation

If the ER stress is too severe, the apoptotic signaling pathways will be activated in the cell[39]. In our scenario this could occur because of the chronic presence of Au NPs that affect the ER functions, and/or because the UPR was impaired and unable to mitigate the protein-folding defects. The redox state of ER is closely related with the protein-folding homeostasis. When oxidative proteins are folded in ER, hydrogen peroxide (H_2O_2) would be generated as a byproduct, since the oxidation of the thiol groups on cysteines of substrate peptides needs to form disulfide bonds[37]. In a ER stress condition, the dysregulated disulfide bond formation would lead to the intracellular reactive (ROS) accumulation and cause oxidative stress, which may ultimately trigger cell apoptosis[37]. Oxidative protein folding or misfolded protein refolding are catalyzed by ER oxidoreductases, *e.g.* protein disulfide isomerases (PDI) and ER oxidoreductase 1 (Ero1, encoded by *ERO1A* and *ERO1B*)[37], which were greatly increased with Au NPs treatment (Fig. 4e and Supplementary Fig. 3d). In addition, to evaluate the oxidative state in cells, we assessed intracellular ROS in cells exposed to Au NPs. A significant increase of intracellular ROS was observed in Au NP-treated cells (Fig. 5a), suggesting an oxidative stress condition. The strong upregulation of the expression of the antioxidant enzyme genes *NQO1* (NADPH Quinone acceptor Oxidoreductase 1), *PRDX1* (Peroxiredoxin 1) and *GPX2* (Glutathione peroxidase 2) further support the Au NP-dependent induction of an intracellular oxidative stress condition (Fig. 5b).

Our data suggest that cell exposure to Au NPs induces the activation of the ER stress-induced apoptotic signaling pathway PERK-eIF2α-ATF4-CHOP. We have therefore evaluated whether exposure to Au NPs could induce cell apoptosis. The results in the Figure 5c show the increase in the number of apoptotic cells (positive to Annexin V in flow cytometry) in cells treated with Au NPs (Fig. 5c). We also argued whether other apoptotic pathways could be involved in the Au NP-induced cell death. Since mitochondria-depended apoptosis signaling pathway has been largely reported as involved in NP-induced apoptosis[2], we have evaluated the expression of a number of mitochondria-associated apoptotic signaling proteins (in particular Bax, Bcl2, cytochrome c, caspase 3/9, PARP), and found no upregulation in their mRNA and protein levels between control and Au NP-treated cells (Fig. 5e-f). These results suggest that the Au NP-

induced cell apoptosis in our study depends on ER stress-induced signaling, and is independent of mitochondria/caspase 3-mediated apoptosis pathways.

The barrier defensive role of epithelial cells is not exclusively mechanical, and they are able to react to stress and challenges by producing and secreting cytokines and chemokines[42]. This is a key process to alert the immune system of any impending danger and initiate the recruitment of immune effector cells[43,44]. Three important inflammation-related factors were evaluated, IL-1α as an alarmin to alert the immune system[45], IL-1β as a key cytokine to activate inflammation and immune effector mechanisms[46], and IL-8 as the key chemokine to recruit neutrophils in the rapid reaction against danger[47]. The results in the Figure 5g show that the secretion of IL-1α, IL-1β and IL-8 was increased as a dose-dependent manner. This implies that exposure to Au NPs could induce ER stress, through PQC dysregulation, promote cell death, and also activate the immune system through the release of alarm and immune-activating factors.

The protein corona mitigates the Au NP-induced effect on the PQC system

Upon interaction with biological fluids, the surface of NPs becomes coated with a layer of biomolecules, mainly proteins (with different composition depending on the biological microenvironment), the protein corona[48], whose presence significantly affects the biological effects of NPs[3,49]. We have previously reported that the presence on Au NPs of a protein corona affected the NP cellular uptake and inflammatory potential[44]. In this study, we have evaluated the effect of the human plasma protein corona on the Au NPs capacity of modulating ER functions and downstream effects. The presence of a protein corona on the surface of Au NPs could be observed by TEM (Fig. 6a). The cytotoxicity of the corona Au NPs was assessed and found to be undetectable (Fig. 6b), at variance with the significant cytotoxicity caused by bare Au NPs (Fig. 1d). The reasons for the lack of cytotoxicity by corona Au NPs was further analyzed. The internalization of Au NPs was significantly decreased in the presence of the corona on Au NPs (Fig. 6c). Since the internalization of Au NPs would largely affect the ER functions, as indicated by our data above, we speculated that the protein coating would also suppress the ER dysfunction and PQC anomalies that bare Au NPs can cause. To this end, we have evaluated ERAD functions by examining the protein stability of CD3-δ and BiP (Fig. 6d-f). The results show that cells treated with corona Au NPs present a quite normal CD3-δ degradation rate, overlapping with that of control cells (Fig. 6e). When compared to bare Au NPs, it is evident that the protein coating on Au NPs abolished the block of CD3-δ degradation (and consequent accumulation) induced in cells by bare Au NPs treatment (Fig. 6f). Likewise, the accelerated BiP degradation induced by cell treatment with bare Au NPs was abolished in cells exposed to corona Au NPs (Fig. 6d-f). We have also examined the corona Au NP effects on UPR and ER stress. Results in the Figure 6g-h show that the levels of BiP, p-eIF2α, eIF2α and *CHOP*, which were increased by cell treatment with bare Au NPs, were all at the level of control cells when Au NPs were coated with a protein corona. The ER stress-induced intracellular ROS, cell apoptosis and cytokine secretion were also assessed and showed to be suppressed when cells treated with the corona Au NPs (Fig. 6i-k).

Discussion

The cytotoxicity of NPs is largely due to the increased production of ROS, and this can depend on ER stress. While there are many publications reporting the NP-associated ER stress, how NPs could cause ER stress and the potential molecular mechanisms underlying it are largely unknown. Proteins, among other key biological macromolecules, need to be tightly controlled in cells, in which ER is the key organelle deputed to biosynthesis, assembly, modification and recycling of proteins. The protein quality control (PQC) system of the ER, works as an essential surveillance mechanism to ensure the proper folding and modification of proteins[50,51]. The effect of NPs on the cellular PQC machinery has never been explored so far. It has been reported that the NPs can change the protein structure extracellularly[24], but nothing is known as to whether the intracellular protein biosynthesis and PQC could be affected by NPs.

In our current study, we have explored the effect of Au NPs on the intracellular levels of misfolded/unfolded proteins, and shown that these are significantly increased in cells treated with Au NPs (Fig. 3a). We may speculate that the internalization of Au NPs in cells may disturb the protein biosynthesis and lead to an increased production of misfolded/unfolded proteins in cells. The increased level of misfolded/unfolded proteins activates the PQC process, which aims to restore the protein homeostasis. In Au NP-treated cells, the PQC activation was shown by the upregulated expression of three chaperones involved in identification and re-shaping of misfolded/unfolded proteins, *i.e.* Hsp70, Hsp90 and BiP (Fig. 3b-c). Since we have identified a preferential localization of Au NPs in the ER (Fig. 2c-e), the same as other reports[20,21], we argued that Au NPs could affect the intracellular PQC through alteration of ERAD, one of the key processes for misfolded/unfolded protein degradation. Indeed, this was the case. As marker substrate of ERAD functions we used CD3-δ, and found its accumulation in cells treated with Au NPs, indicative of an impairment of the ERAD mechanism of protein elimination (Fig. 3d-e). This is the first evidence ever that Au NPs can interfere with the PQC process in the ER. The chaperone BiP, which is active in the ER, was observed to be unstable and insufficient, with an accelerated degradation in cells treated with Au NPs (Fig. 3d-e and Supplementary Fig. 2a-c). Therefore, these results suggested that in Au NP-treated cells two phenomena occur, the accumulation of misfolded/unfolded proteins and the impaired capacity of identifying and correcting them (impaired ERAD). The impaired ERAD would result in an excessive accumulation of misfolded/unfolded proteins in the ER lumen and membrane, and lead to a condition known as ER stress, a phenomenon observed in several diseases[52].

Cells have a tightly controlled intracellular regulatory network to modulate relevant signaling pathways for the protein homeostasis recovery. In the presence of misfolded/unfolded proteins, the UPR signaling pathway, a kinase-mediated phosphorylation cascade, can be activate to alleviate the stress condition[10-13]. PERK, ATF6α and IRE1, the three UPR sensors, can detect the misfolded/unfolded proteins and transduce signals from the ER to the nucleus for activating genes and inducing production of proteins aiming at restoring ERAD functions and eliminate ER stress. The presence of misfolded/unfolded proteins induced the dimerization and auto-phosphorylation of IRE1, an ER membrane integral protein, activating the endonuclease activity of its cytosolic domain, which in turn splices the ubiquitous cytosolic

mRNA of *XBP1* into *sXBP1*, which will generate the active sXBP1 protein[53]. This is a transcription factor that will further activate the expression of chaperone and ERAD genes for re-establishing misfolded/unfolded proteins degradation[33]. In a more severe conditions, PERK and the PERK-eIF2α-ATF4-CHOP signaling pathway would be activated to clear the misfolded/unfolded proteins and, if the severe conditions persist, to eventually induce cell apoptosis[54]. All these events are part of the ER stress condition[55]. To investigate the UPR signaling and ER stress, the expression of the main signaling pathway genes was assessed by a PCR array and showed the induction of an active UPR and ER stress condition in cells treated with Au NPs (Fig. 4). The spliced and unspliced forms of XBP1 (*sXBP1* and *usXBP1*), as well as PERK pathway genes, were all identified as upregulated.

If the accumulation of misfolded/unfolded proteins and the ER stress persist, intracellular ROS would be generated, since the ER dysfunction would also lead to misfolding of oxidative proteins with the generation of H_2O_2 as a byproduct[37,56]. *PDI*, *ERO1A* and *ERO1B*, the ER oxidoreductases and the downstream genes of the pro-apoptotic gene of *CHOP*, all were activated in cells treated with Au NPs (Fig. 4 and Supplementary Fig. 3), a finding that implies the breakdown of the intracellular redox balance. Intracellular ROS level and cell apoptosis were also evaluated and found increased in cells treated Au NPs (Fig. 5a-d).

Our data indicate NP-induced ER stress as a new pathway by which NPs can induce intracellular ROS, other than the well-known NP-mediated mitochondria-ROS-apoptosis pathway[2]. To examine the possible involvement of the mitochondria-related pathway, we have also assessed the expression of relevant signaling molecules, and found that treatment with Au NPs was unable to activate them in cells (Fig. 5e-f).

The formation of a protein corona on NPs upon contact with biological fluids/systems can greatly influence the NP-induced biological effects[57]. It has been shown that the formation of a protein corona on the surface of graphene oxide inhibited the NP-induced cell damage and death[58]. However, in another study the presence of a protein corona strongly increased the ER stress induced by silver NPs[59]. Because of these contradictory results, we have also assessed the protein corona effects of NPs on the PQC system. We clearly show that the NP internalization is significantly decreased in the presence of protein corona (Fig. 6c), a fact that can mitigate the Au NP-induced intracellular accumulation of misfolded/unfolded proteins, as well as the PQC system (Fig. 6d-f). Thus, the intracellular ROS, cell apoptosis and overall cytotoxicity were greatly inhibited in cells exposed to corona Au NPs. It is also possible that the masking of the reactive NP surface by the protein corona could inhibit the interaction of NPs with the ER functional proteins, thereby preventing a direct NP-induced PQC dysfunction and ER stress[36]. Therefore, we believe that the amount of intracellular NP and their interaction with ER are the keys for NP-induced PQC dysfunction. Actually, Au NPs with negative surface charge (*e.g.* citrate coating and lipoic acid coating) cannot be internalized in a high volume[19], which merely induce a significant accumulation of misfolded/unfolded protein and PQC dysfunction (data not show). Since many molecules of PQC have already been used as targets for disease therapy (cancer or Alzheimer's disease)[7-

[9], our study also reveals a new strategy for the design of smart nanomedicine that targeting ER and intracellular PQC.

Epithelial cells, in its important barrier and defensive role, are able to secrete many cytokines and chemokines to alarm the immune system of potential danger and recruit immune effector cells[27,60]. A robust protein biosynthesis requires a fully functional PQC system in cells. Because of the NP-induced PQC alternations, we were hypothesizing a possible impairment also in the cytokine and chemokine synthesis and secretion capacity in cells. However, we could detect an increased cytokine/chemokine secretion (Fig. 5g), which implies that the protein synthesis capacity of ER was not affected by the internalized Au NPs and the alarming function of the epithelial cells was not inhibited but actually enhanced in cells treated with Au NPs. There are however many reports on the capacity of NPs to inhibit inflammatory responses, measured in terms of decreased cytokine secretion[61-63]. It would be tempting to speculate that in those cases the inhibition of cytokine production could be consequence of the NP-hampered ER functions and protein synthesis capacity, a possibility that needs investigation.

Conclusions

This study investigated for the first time the possible molecular mechanisms underlying the NP-induced ER stress, and presented evidence that NPs can interfere with the PQC system thereby triggering ER stress. The ER location of Au NPs correlated with ER dysfunction with the subsequent hampering of the intracellular PQC functions, as shown by the accumulation of misfolded/unfolded proteins and ERAD impairment. These alterations triggered ER stress, with consequent intracellular ROS accumulation and ultimately causing cell apoptosis through the activation of the IRE1 and PERK signaling pathways (mechanism illustrated in Fig. 7).

Materials And Methods

Au NPs and the preparation of corona Au NPs

Forty nm BPEI-coated Au NPs, synthesized by the hydrogen tetrachloroaurate (III) reduction method as reported previously[44], were purchased from nanoComposix (San Diego, CA, USA) and kept stored at 4°C in the dark. Endotoxin contamination was evaluated with previously reported LAL-based modified methods, and shown to be less than 2.0 EU/mg[64]. FITC-functionalized Au NPs were synthesized as previously described[65]. In brief, 100 µl FITC-NHS (N-hydroxysuccinimide) (1 mg/ml) were added into 5 ml BPEI-Au NPs (1 mg/ml) in water. The reaction mixture was stirred at 4°C overnight. The FITC-BPEI-Au NPs were collected by centrifugation at 12,000 rpm for 10 min, and washed 3x with endotoxin-free cell culture grade water. The obtained FITC-BPEI-Au NPs were stored at 4°C in the dark.

Pooled human plasma was bought from Biological Specialty Corp. (Colmar, PA, USA). As indicated by the company, human blood was collected with anti-coagulating reagents from healthy donors (n=5), and centrifuged at room temperature (RT) to obtain human plasma. Au NPs were incubated with 55% v/v

human plasma (with PBS) in an orbital shaking incubator for 1 h at 450 rpm at 37°C. Plasma-NP complexes were washed 3x with PBS to remove the weakly associated proteins (known as “soft protein corona”), and centrifuged for 15 min at 20,000 g at 18°C. The final protein-coated Au NPs (with “hard protein corona” and known as “corona Au NPs” in this study) were re-suspended in PBS.

NP characterization

Au NPs, either bare or coated with human plasma proteins (corona Au NPs), were characterized by transmission electron microscopy (TEM) with a FEI Tecnai G2 Spirit BioTWIN TEM (FEI, Hillsboro, OR, USA). The hydrodynamic diameter and zeta potential were detected by the Zetasizer Nano ZS (Malvern Instruments, Worcester, UK). The UV-VIS spectrophotometrical profile was detected with a BioTek Hybrid reader (BioTek Instruments, Inc., Winooski, VT, USA). The reported results of size distribution and zeta potential were obtained with 4 measurements for 10 counts each. The fluorescence emission band of FITC-Au NPs was detected by the Edinburgh Instruments, FS920 (Edinburgh Instruments, UK).

Cell culture

Cryopreserved primary human epidermal keratinocytes (HEK) were obtained from Lonza (Walkersville, MD, USA), and human mammary adenocarcinoma MCF7 cells were obtained from ATCC (Manassas, VA, USA). HEK and MCF7 cells were cultured in DMEM (HyClone, Logan, UT, USA) supplemented with 10% foetal bovine serum (FBS; Gibcoâ, Thermo Fisher Scientific, Inc., Waltham, MA, USA) and 1% penicillin/streptomycin solution (stock concentration as 10,000 units/ml of penicillin and 10 mg/ml streptomycin; Hyclone) at 37°C in humidified atmosphere with 5% CO_2.

Cell viability assay

HEK cells were exposed to bare or corona Au NPs at the concentrations of 6.25, 12.5 25, 50, 75, 100, 150 and 200 µg/ml (6 wells per condition) in 96-well plates. After 24 h incubation, cells were washed 3x with PBS, and medium with Alamar blue (1:10 volume ratio) was added to each well and incubated for 3 h at 37°C. The cell-permeable non-fluorescent blue compound resazurin, contained in the Alamar blue solution, is reduced intracellularly to fluorescent red resorufin by living cells. Fluorescence, which correlates with cell viability, was detected at 545 nm/590 nm excitation/emission with a BioTek Hybrid reader (BioTek Instruments, Inc.). Cell viability was calculated by normalizing the treated cells to the controls and expressed as percent viability. The half maximal inhibitory concentration 50 (IC50) was calculated by OriginPro 8 with non-lineal curve fitting (Category: pharmacology; Function: dose response) as: *y= 1.05231/(1+10^(-0.024 * (71.34763-x)))-0.04395*, in which *y* represents cell viability and *x* represents concentration.

ICP-MS analysis on Au NP cellular uptake

HEK cells were seeded in 6 well-plates at a density of 2.5 x 10^6 cells/well. Bare and corona Au NPs were added to cells at 25 µg/ml and incubated for 24 h. Cells were washed 3x with PBS and then subjected to

an etching process with 1 ml I_2/KI (0.34 mM/2.04 mM) for 3 min to remove the surface attached Au NPs[66]. After etching, cells were washed 3x with PBS and collected for ICP-MS analysis. The preparation of ICP-MS samples and the ICP-MS detection were performed based on a standard operation procedure for gold ions, and the internalization amount of Au NPs in cells was calculated as for number of NPs. All detailed methods can be found in previous publications[44].

Transmission electron microscopy (TEM)

TEM characterization of Au NPs: A drop of Au NPs was placed on a formvar-coated carbon grid and air dried, then observed with a FEI Tecnai G2 Spirit BioTWIN TEM (FEI, Hillsboro, OR, USA) at an accelerating voltage of 120 kV.

TEM observation of Au NPs uptake: HEK cells were grown to 80% confluency and exposed to 25 µg/ml Au NPs for 24 h. Cells then were collected and fixed for 24 h in 4% formaldehyde and 1% glutaraldehyde in phosphate buffer, followed by rinsing in 0.1 M phosphate buffer. Cell pellets were embedded in 3% agar and post-fixed in 1% osmium tetroxide for 1 h. After washing and centrifugation, cell pellets were dehydrated in ethanol, cleared in acetone, infiltrated and embedded in Spurr's resin (Polysciences, Inc., Warrington, PA, USA). Thin sections of 800A˚ were mounted on copper grids and examined unstained with a FEI Tecnai G2 Spirit BioTWIN TEM with 80 kV accelerating voltage.

Confocal microscopy

The co-localization of ER and Au NPs was examined in HEK cells by confocal microscopy. Briefly, cells at a density of $1x10^5$ cells/well were seeded in confocal microscopy dishes and incubated for 24 h. Cells were treated with 50 µg/ml of FITC-functionalized Au NPs for additional 24 h at 37°C, then washed 3x PBS, and incubated with ER-Tracker™ Blue-White DPX dye (Thermo Fisher Scientific, Inc.) for 15 min at 37°C for ER labelling. Treated cells were fixed and observed with a confocal laser scanning microscope (Leica SD AF, Wetzlar, Germany).

Cell transfection and ERAD analysis

CD3-δ transfection was performed based on previous publication[67]. Cells were transfected with CD3-δ-YFP (labelled with fluorescent YFG), and the transfection rate was evaluated by fluorescence microscopy. Since HEK are primary epithelial cells, the transfection rate of CD3-δ was very low and could not be detected successfully (data not shown). Thus, MCF7, a transformed epithelial tumor cell line, was used for CD3-δ transfection. As validity control, we have assessed the biological effects of Au NP treatment on PQC and other related functions. The results reported in the Supplementary Fig. 4, confirm that Au NPs have on MCF7 cells the same effects as on HEK cells, making them a suitable HEK proxy for examining ERAD functions.

In brief, cells were seeded in 12-well plates at a density of $3x10^5$ cells/well/ml overnight. Cells were then transfected by 0.5 mg CD3-δ-YFP with lipofectamine 2000 (Thermo Fisher Scientific, Inc.) for 24 h,

obtaining a transfection rate of over 80%. Culture medium was then replaced with fresh medium containing 10 μg/ml Au NPs (either bare or corona Au NPs) or 1 μM thapsigargin (TG) for 24 h. Cycloheximide (CHX; 10 μM) was added from time 18 h for 2, 4 and 6 h, to block protein synthesis and allow for examining the time course of protein degradation. Cells without CHX were used as control. The results were calculated based on the gray value that measured by ImageJ. The levels of BiP and CD3-δ was first normalized *vs.* GAPDH at each time point, and then expressed as fold change *vs.* time 0.

Western blot analysis

After different treatments, cells were washed 3x with cooled PBS and lysed in RIPA lysis buffer containing 1x complete protease inhibitor cocktail for 30 min on ice, then centrifuged at 15,000 g for 5 min at 4°C. Cell debris pellets were collected for misfolded and unfolded protein analysis. Supernatants were also collected for quantitative protein analysis. Protein concentrations were measured by BCA assay (Boster Biological Technologies Co., Ltd., Wuhan, P.R. China). Samples were boiled with loading buffer at 100°C for 5 min and run on SDS-PAGE. Proteins were detected with specific antibodies as indicated in the Figures. Antibodies were all obtained from Cell Signaling Technology, Inc. (Danvers, MA, USA).

Intracellular ROS detection

Cells were seeded in 6-well plates at a density of $3x10^6$ cells/well, and incubated for 24 h in the presence or absence of 75 μg/ml Au NPs. H_2O_2 (200 mM) was used as positive control in a 3 h treatment. Cells were then washed 3x with PBS to eliminat the Au NPs, incubated with the cell permeant fluorogenic dye CM-H_2DCFDA (10 mM) for 30 min, and washed 3x with PBS to eliminate the excess unreacted DCFDA. Fluorescence, generated by the ROS-dependent oxidation of DCFDA metabolites into the fluorescent compound DCF, was detected cytofluorimetrically with excitation of 488 nm. Results were analysed with FlowJo and presented either as histogram or fold change by normalizing the treated cells to controls[2].

Human molecular pathway finder PCR array

HEK cells were seeded in T-25 flasks at a density of $5x10^5$ cells per flask and incubated for 24 h at 37°C in air with 5% CO_2. Medium was replaced with fresh medium (control) or medium containing 25 μg/ml or 75 μg/ml Au NPs in triplicate samples. After 24 h incubation, cells were washed 3x with PBS and collected for RT² Profiler™ PCR Array Human Molecular Toxicology PathwayFinder 384HT (Qiagen, Hilden, Germany) analysis. A detailed method is attached in supporting information.

Quantitative RT-PCR analysis

After different treatments, cells were washed 3x with cooled PBS and lysed with RNA plus (Takara Bio, Inc., Otsu, Japan) for total RNA extraction. RNA (1 μg) was reverse-transcribed with the PrimeScript RT Reagent Kit with gDNA Eraser Kit (Takara Bio, Inc.). Quantitative RT-PCR was performed using the SYBR Green PCR Master Mix (Takara Bio, Inc.). GAPDH was used as housekeeping gene. The calculation

methods is described in the supporting information. Primer sequences were synthesized by Sangon Biotech (Shanghai, China) (see the Supplement Table 1). Unlisted primers were bought from Qiagen.

Apoptosis evaluation

Cells were seeded in 6-well plates at a density of $3x10^6$ cells/well and incubated in the presence or absence of Au NPs for 24 h. Cells were detached with trypsin, and the FITC Apoptosis Detection Kit I (BD Biosciences, Franklin Lakes, NJ, USA) was used for evaluating the number of apoptotic cells. Cells were incubated with Annexin V (FITC) and propidium iodide (PI) at RT for 15 min and then assessed by flow cytometry. Results were analyzed with FlowJo. Cells negative for both PI and Annexin V staining were considered alive; cells positive for Annexin V were considered as apoptotic (Annexin V single positive, Annexin V and PI double positive); and cells only positive for PI were considered as necrotic.

Cytokine production

HEK cells were treated with 25 and 75 µg/ml of Au NPs for 24 h. Supernatants were collected, and IL-1α, IL-1β and IL-8 were quantitated by enzyme-linked immunosorbent assay (ELISA), with commercially available kits (R&D Systems, Minneapolis, MN, USA), according to the manufacturer's instructions.

Statistical analysis

Results are presented as mean values of replicate experiments or replicate samples within one representative experiment as indicated in the Figure legends. Statistically significant differences (p <0.05) were determined with the Student's t-test and ANOVA.

References

1 Nel, A., Xia, T., Mädler, L. & Li, N. Toxic potential of materials at the nanolevel. *Science* **311**, 622-627 (2006).

2 Li, Y. *et al.* The triggering of apoptosis in macrophages by pristine graphene through the MAPK and TGF-beta signaling pathways. *Biomaterials* **33**, 402-411 (2012).

3 Salvati, A. *et al.* Transferrin-functionalized nanoparticles lose their targeting capabilities when a biomolecule corona adsorbs on the surface. *Nat. Nanotechnol.* **8**, 137-143 (2013).

4 Sauvage, F. *et al.* Nanomaterials to avoid and destroy protein aggregates. *Nano Today*, 100837 (2020).

5 Chen, B., Retzlaff, M., Roos, T. & Frydman, J. Cellular strategies of protein quality control. *Cold Spring Harb. Perspect. Biol.* **3**, a004374 (2011).

6 Wu, J. & Kaufman, R. J. From acute ER stress to physiological roles of the Unfolded Protein Response. *Cell Death Differ* **13**, 374-384, doi:10.1038/sj.cdd.4401840 (2006).

7 de Vrij, F. M., Fischer, D. F., van Leeuwen, F. W. & Hol, E. M. Protein quality control in Alzheimer's disease by the ubiquitin proteasome system. *Progress in neurobiology* **74**, 249-270, doi:10.1016/j.pneurobio.2004.10.001 (2004).

8 Schönthal, A. H. Endoplasmic reticulum stress and autophagy as targets for cancer therapy. *Cancer Letters* **275**, 163-169, doi:https://doi.org/10.1016/j.canlet.2008.07.005 (2009).

9 Dubnikov, T., Ben-Gedalya, T. & Cohen, E. Protein Quality Control in Health and Disease. *Cold Spring Harb Perspect Biol* **9**, doi:10.1101/cshperspect.a023523 (2017).

10 Hwang, J. & Qi, L. Quality Control in the Endoplasmic Reticulum: Crosstalk between ERAD and UPR pathways. *Trends Biochem Sci* **43**, 593-605, doi:10.1016/j.tibs.2018.06.005 (2018).

11 Haze, K., Yoshida, H., Yanagi, H., Yura, T. & Mori, K. Mammalian transcription factor ATF6 is synthesized as a transmembrane protein and activated by proteolysis in response to endoplasmic reticulum stress. *Mol Biol Cell* **10**, 3787-3799, doi:10.1091/mbc.10.11.3787 (1999).

12 Mori, K., Ma, W. Z., Gething, M. J. & Sambrook, J. A Transmembrane Protein with a Cdc2+/Cdc28-Related Kinase-Activity Is Required for Signaling from the Er to the Nucleus. *Cell* **74**, 743-756 (1993).

13 Shi, Y. *et al.* Identification and characterization of pancreatic eukaryotic initiation factor 2 alpha-subunit kinase, PEK, involved in translational control. *Mol Cell Biol* **18**, 7499-7509, doi:10.1128/mcb.18.12.7499 (1998).

14 Buchberger, A., Bukau, B. & Sommer, T. Protein quality control in the cytosol and the endoplasmic reticulum: brothers in arms. *Mol cell* **40**, 238-252, doi:10.1016/j.molcel.2010.10.001 (2010).

15 Nishikawa, S., Brodsky, J. L. & Nakatsukasa, K. Roles of molecular chaperones in endoplasmic reticulum (ER) quality control and ER-associated degradation (ERAD). *J Biochem* **137**, 551-555, doi:10.1093/jb/mvi068 (2005).

16 Terrab, L. & Wipf, P. Hsp70 and the Unfolded Protein Response as a Challenging Drug Target and an Inspiration for Probe Molecule Development. *ACS Med Chem Lett.* **11**, 232-236, doi:10.1021/acsmedchemlett.9b00583 (2020).

17 Sperling, R. A., Gil, P. R., Zhang, F., Zanella, M. & Parak, W. J. Biological applications of gold nanoparticles. *Chem. Soc. Rev.* **37**, 1896-1908 (2008).

18 Yen, H. J., Hsu, S. h. & Tsai, C. L. Cytotoxicity and immunological response of gold and silver nanoparticles of different sizes. *Small* **5**, 1553-1561 (2009).

19 Li, Y. *et al.* Assessing the Immunosafety of Engineered Nanoparticles with a Novel in vitro Model Based on Human Primary Monocytes. *ACS Appl. Mater. Interfaces* **8 (42)**, 28437–28447, doi:10.1021/acsami.6b06278 (2016).

20 Chang, M. Y. *et al.* Increased apoptotic potential and dose-enhancing effect of gold nanoparticles in combination with single-dose clinical electron beams on tumor-bearing mice. *Cancer Sci* **99**, 1479-1484, doi:10.1111/j.1349-7006.2008.00827.x (2008).

21 Pan, T. *et al.* miR-29b-Loaded Gold Nanoparticles Targeting to the Endoplasmic Reticulum for Synergistic Promotion of Osteogenic Differentiation. *ACS Appl Mater Interfaces* **8**, 19217-19227, doi:10.1021/acsami.6b02969 (2016).

22 Noël, C., Simard, J.-C. & Girard, D. Gold nanoparticles induce apoptosis, endoplasmic reticulum stress events and cleavage of cytoskeletal proteins in human neutrophils. *Toxicology in Vitro* **31**, 12-22 (2016).

23 Tsai, Y. Y. *et al.* Identification of the nanogold particle-induced endoplasmic reticulum stress by omic techniques and systems biology analysis. *ACS nano* **5**, 9354-9369, doi:10.1021/nn2027775 (2011).

24 Deng, Z. J., Liang, M., Monteiro, M., Toth, I. & Minchin, R. F. Nanoparticle-induced unfolding of fibrinogen promotes Mac-1 receptor activation and inflammation. *Nat. Nanotechnol.* **6**, 39-44 (2011).

25 Shang, L., Wang, Y., Jiang, J. & Dong, S. pH-dependent protein conformational changes in albumin: gold nanoparticle bioconjugates: a spectroscopic study. *Langmuir* **23**, 2714-2721 (2007).

26 Tsai, D.-H. *et al.* Adsorption and conformation of serum albumin protein on gold nanoparticles investigated using dimensional measurements and in situ spectroscopic methods. *Langmuir* **27**, 2464-2477 (2011).

27 Janeway, C. A., Capra, J. D., Travers, P. & Walport, M. *Immunobiology: the immune system in health and disease*. (1999).

28 Li, Y. & Boraschi, D. Endotoxin contamination: a key element in the interpretation of nanosafety studies. *Nanomedicine (Lond)* **11**, 269-287, doi:10.2217/nnm.15.196 (2016).

29 Murali, K. *et al.* Uptake and bio-reactivity of polystyrene nanoparticles is affected by surface modifications, ageing and LPS adsorption: in vitro studies on neural tissue cells. *Nanoscale* **7**, 4199-4210 (2015).

30 Li, Y., Fujita, M. & Boraschi, D. Endotoxin contamination in nanomaterials leads to the misinterpretation of immunosafety results. *Front. Immunol.* **8**, doi:10.3389/fimmu.2017.00472 (2017).

31 Komander, D. & Rape, M. The ubiquitin code. *Annu Rev Biochem* **81**, 203-229, doi:10.1146/annurev-biochem-060310-170328 (2012).

32 Chen, L., Zhu, G., Johns, E. M. & Yang, X. TRIM11 activates the proteasome and promotes overall protein degradation by regulating USP14. *Nat. Commun.* **9**, 1-14 (2018).

33 Buchberger, A., Bukau, B. & Sommer, T. Protein quality control in the cytosol and the endoplasmic reticulum: brothers in arms. *Mol cell* **40**, 238-252 (2010).

34 Menendez-Benito, V., Verhoef, L. G., Masucci, M. G. & Dantuma, N. P. Endoplasmic reticulum stress compromises the ubiquitin–proteasome system. *Hum. Mol. Genet.* **14**, 2787-2799 (2005).

35 Yang, M., Omura, S., Bonifacino, J. S. & Weissman, A. M. Novel aspects of degradation of T cell receptor subunits from the endoplasmic reticulum (ER) in T cells: importance of oligosaccharide processing, ubiquitination, and proteasome-dependent removal from ER membranes. *J. Exp. Med.* **187**, 835-846 (1998).

36 Amen, O. M., Sarker, S. D., Ghildyal, R. & Arya, A. Endoplasmic reticulum stress activates unfolded protein response signaling and mediates inflammation, obesity, and cardiac dysfunction: therapeutic and molecular approach. *Front. Pharmacol.* **10** (2019).

37 Cao, S. S. & Kaufman, R. J. Endoplasmic reticulum stress and oxidative stress in cell fate decision and human disease. *Antioxid Redox Signal* **21**, 396-413, doi:10.1089/ars.2014.5851 (2014).

38 Tabas, I. & Ron, D. Integrating the mechanisms of apoptosis induced by endoplasmic reticulum stress. *Nat. Cell Biol.* **13**, 184-190 (2011).

39 Hetz, C. The unfolded protein response: controlling cell fate decisions under ER stress and beyond. *Nat Rev Mol Cell Biol* **13**, 89-102, doi:10.1038/nrm3270 (2012).

40 Yoshida, H., Oku, M., Suzuki, M. & Mori, K. pXBP1(U) encoded in XBP1 pre-mRNA negatively regulates unfolded protein response activator pXBP1(S) in mammalian ER stress response. *J Cell Biol* **172**, 565-575, doi:10.1083/jcb.200508145 (2006).

41 Okuda-Shimizu, Y. & Hendershot, L. M. Characterization of an ERAD pathway for nonglycosylated BiP substrates, which require Herp. *Mol cell* **28**, 544-554 (2007).

42 Larsen, S. B., Cowley, C. J. & Fuchs, E. Epithelial cells: liaisons of immunity. *Curr Opin Immunol* **62**, 45-53, doi:10.1016/j.coi.2019.11.004 (2020).

43 Kagnoff, M. F. & Eckmann, L. Epithelial cells as sensors for microbial infection. *J. Clin. Invest.* **100 (1)**, 6-10 (1997).

44 Li, Y. & Monteiro-Riviere, N. A. Mechanisms of cell uptake, inflammatory potential and protein corona effects with gold nanoparticles. *Nanomedicine* **11**, 3185-3203 (2016).

45 Werman, A. *et al.* The precursor form of IL-1α is an intracrine proinflammatory activator of transcription. *Proc. Natl. Acad. Sci. U. S. A.* **101**, 2434-2439 (2004).

46 Rider, P. *et al.* IL-1α and IL-1β recruit different myeloid cells and promote different stages of sterile inflammation. *J. Immunol.* **187**, 4835-4843 (2011).

47 Kunkel, S. L., Standiford, T., Kasahara, K. & Strieter, R. M. Interleukin-8 (IL-8): the major neutrophil chemotactic factor in the lung. *Experimental lung research* **17**, 17-23 (1991).

48 Lynch, I., Salvati, A. & Dawson, K. A. Protein-nanoparticle interactions: what does the cell see? *Nat. Nanotechnol.* **4**, 546-547 (2009).

49 Monopoli, M. P. *et al.* Physical-chemical aspects of protein corona: relevance to in vitro and in vivo biological impacts of nanoparticles. *Journal of the American Chemical Society* **138**, 2525–2534 (2011).

50 Comyn, S. A., Chan, G. T. & Mayor, T. False start: cotranslational protein ubiquitination and cytosolic protein quality control. *J Proteomics* **100**, 92-101, doi:10.1016/j.jprot.2013.08.005 (2014).

51 Amm, I., Sommer, T. & Wolf, D. H. Protein quality control and elimination of protein waste: the role of the ubiquitin-proteasome system. *Biochim Biophys Acta* **1843**, 182-196, doi:10.1016/j.bbamcr.2013.06.031 (2014).

52 Ruggiano, A., Foresti, O. & Carvalho, P. ER-associated degradation: Protein quality control and beyond. *J. Cell Biol.* **204**, 869-879 (2014).

53 Yoshida, H., Matsui, T., Yamamoto, A., Okada, T. & Mori, K. XBP1 mRNA is induced by ATF6 and spliced by IRE1 in response to ER stress to produce a highly active transcription factor. *Cell* **107**, 881-891 (2001).

54 Li, Y., Guo, Y., Tang, J., Jiang, J. & Chen, Z. New insights into the roles of CHOP-induced apoptosis in ER stress. *Acta biochimica et biophysica Sinica* **46**, 629-640 (2014).

55 Sano, R. & Reed, J. C. ER stress-induced cell death mechanisms. *Biophys. Acta, Mol. Cell Res.* **1833**, 3460-3470 (2013).

56 Fu, P. P., Xia, Q., Hwang, H. M., Ray, P. C. & Yu, H. Mechanisms of nanotoxicity: generation of reactive oxygen species. *J Food Drug Anal* **22**, 64-75, doi:10.1016/j.jfda.2014.01.005 (2014).

57 Corbo, C. *et al.* The impact of nanoparticle protein corona on cytotoxicity, immunotoxicity and target drug delivery. *Nanomedicine* **11**, 81-100 (2016).

58 Hu, W. *et al.* Protein corona-mediated mitigation of cytotoxicity of graphene oxide. *ACS Nano* **5**, 3693-3700, doi:10.1021/nn200021j (2011).

59 Persaud, I. *et al.* Biocorona formation contributes to silver nanoparticle induced endoplasmic reticulum stress. *Ecotoxicol Environ Saf* **170**, 77-86, doi:10.1016/j.ecoenv.2018.11.107 (2019).

60 Quaresma, J. A. S. Organization of the Skin Immune System and Compartmentalized Immune Responses in Infectious Diseases. *Clin Microbiol Rev* **32**, e00034-00018, doi:10.1128/CMR.00034-18 (2019).

61 Tian, M. *et al.* Adipose-Derived Biogenic Nanoparticles for Suppression of Inflammation. *Small* **16**, e1904064, doi:10.1002/smll.201904064 (2020).

62 Crisan, D. *et al.* Topical silver and gold nanoparticles complexed with Cornus mas suppress inflammation in human psoriasis plaques by inhibiting NF-kappaB activity. *Exp Dermatol* **27**, 1166-1169, doi:10.1111/exd.13707 (2018).

63 Kim, J. H. *et al.* Immunotoxicity of silicon dioxide nanoparticles with different sizes and electrostatic charge. *Int J Nanomedicine* **9 Suppl 2**, 183-193, doi:10.2147/IJN.S57934 (2014).

64 Li, Y. *et al.* Optimising the use of commercial LAL assays for the analysis of endotoxin contamination in metal colloids and metal oxide nanoparticles. *Nanotoxicology* **9**, 462-473 (2015).

65 Feshitan, J. A., Vlachos, F., Sirsi, S. R., Konofagou, E. E. & Borden, M. A. Theranostic Gd (III)-lipid microbubbles for MRI-guided focused ultrasound surgery. *Biomaterials* **33**, 247-255 (2012).

66 Cho, E. C., Xie, J., Wurm, P. A. & Xia, Y. Understanding the role of surface charges in cellular adsorption versus internalization by selectively removing gold nanoparticles on the cell surface with a I2/KI etchant. *Nano letters* **9**, 1080-1084 (2009).

67 Liu, Y. *et al.* TRIM25 promotes the cell survival and growth of hepatocellular carcinoma through targeting Keap1-Nrf2 pathway. *Nat. Commun.* **11**, 1-13 (2020).

Declarations

Acknowledgements

We thank Nico Dantuma (Karolinska Institutet, Stockholm, Sweden) for providing the CD3-δ-YFP plasmid.

Author Contributions

Y.L. conceived and designed the project. Y.L., Y.C. and H.L. supervised the study. G.Z., Q.S., Y.Z., R.L., Y.L. performed experiments, Y.L., H.L., Y.C., D.B., L.C., N.A.M and G.Z. analyzed and discussed the data. Y.L. D.B. and G.Z. wrote the manuscript. ‡These authors contributed equally.

Competing Interests

The authors declare no competing financial interests.

Funding Sources

This study was supported by the National Natural Science Foundation of China (31701005, 31801186, 81903177), CAS PIFI (2020VBA0028) and SIAT Innovation Program for Excellent Young Researchers (201802).

Table 1

Table 1. Characterization of Au NPs with and without protein corona.

Au NPs	Hydrodynamic diameter (nm)	Polydispersity Index	Z-potential (mV)
Bare	50.8 ± 0.5	0.193	64.1
Protein corona	385.3 ± 23.75	0.386	-13.6

PdI: polydispersity index

Figures

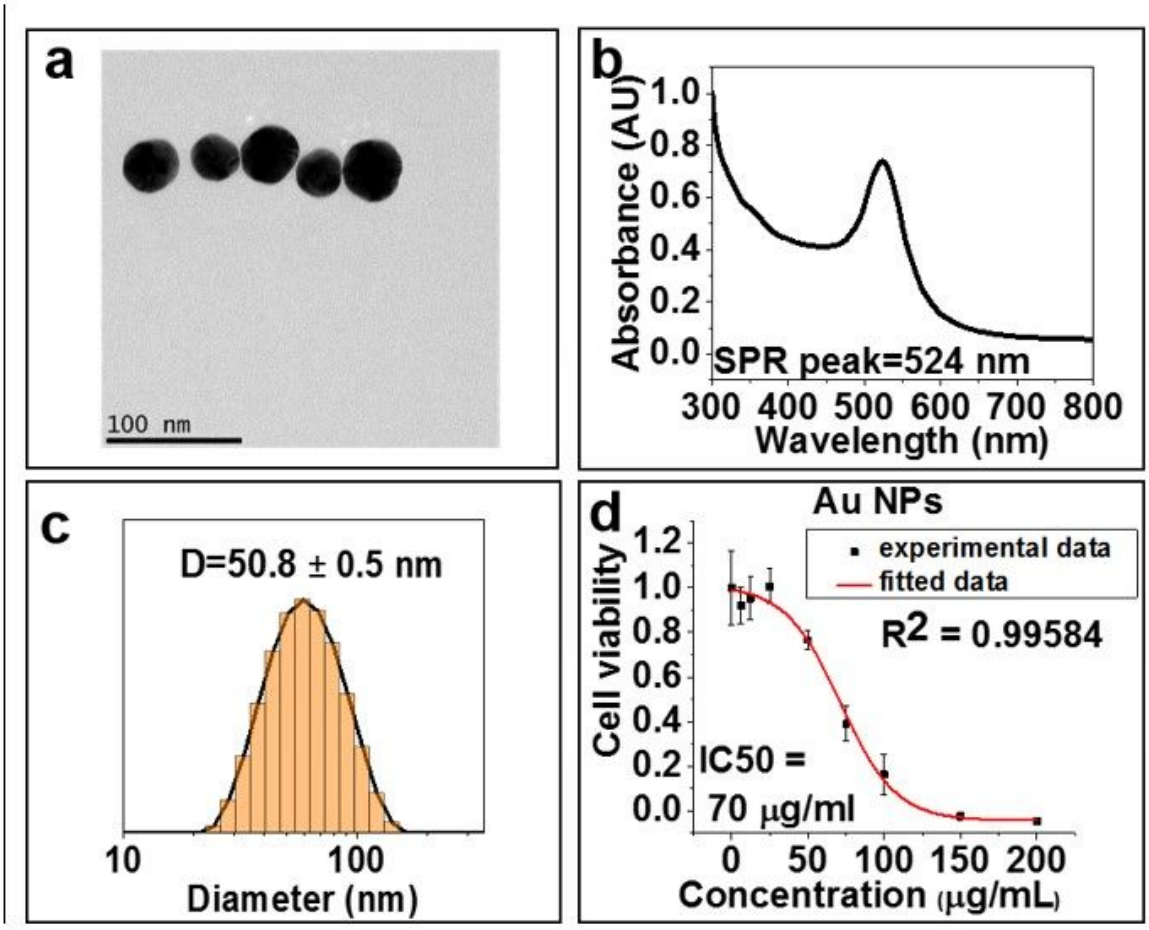

Figure 1

The physicochemical and biological characterization of Au NPs. a TEM image; b the UV-VIS spectrum; c the size distribution evaluated by DLS of Au NPs; and d cell viability upon cells exposure to Au NPs. Cells were exposed to various concentrations of Au NPs for 24 h and the cell viability was evaluated with Alamar blue. Data were analyzed with linear regression analysis, and the half maximal inhibitory concentration (IC50) was calculated.

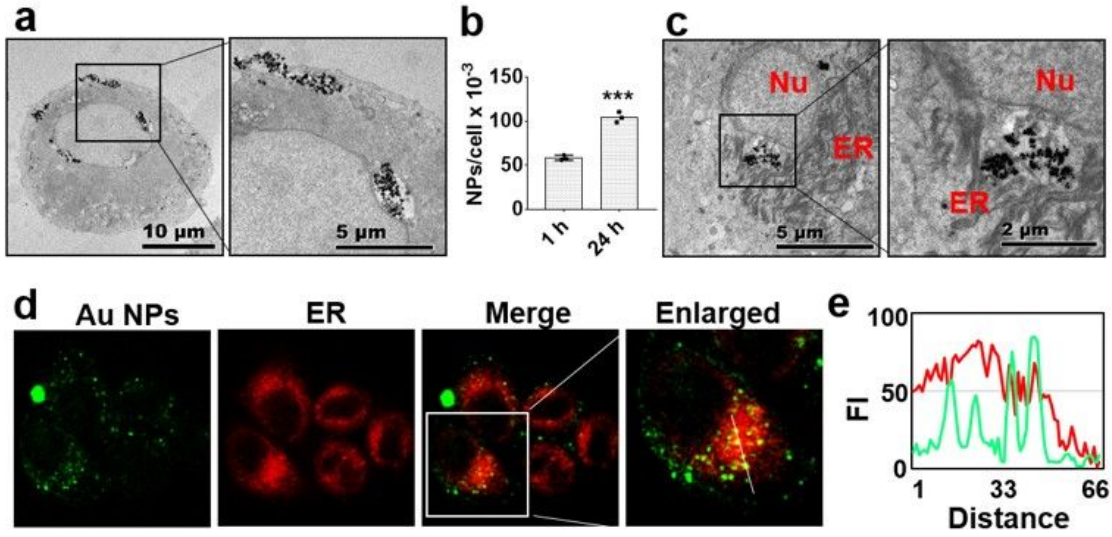

Figure 2

Internalization and subcellular localization of Au NPs. Cells were exposed to Au NPs for 24 h. a TEM images depicting the internalization of Au NPs. b Quantitative evaluation of intracellular Au NPs at 1 and 24 h, assessed by ICP-MS. Data are presented as mean ± SEM of triplicate samples. ***, $p<0.005$ vs. 1 h. c Subcellular localization of Au NPs observed by TEM. Nu: nucleus; ER: endoplasmic reticulum. d Intracellular localization of Au NPs observed by confocal microscopy. Green: FITC-labeled Au NPs; Red: ER-Tracker™ Blue-White DPX dye stained ER. e Fluorescence intensity (FI) profiles measured on the line labeled in white in the enlarged image in panel d.

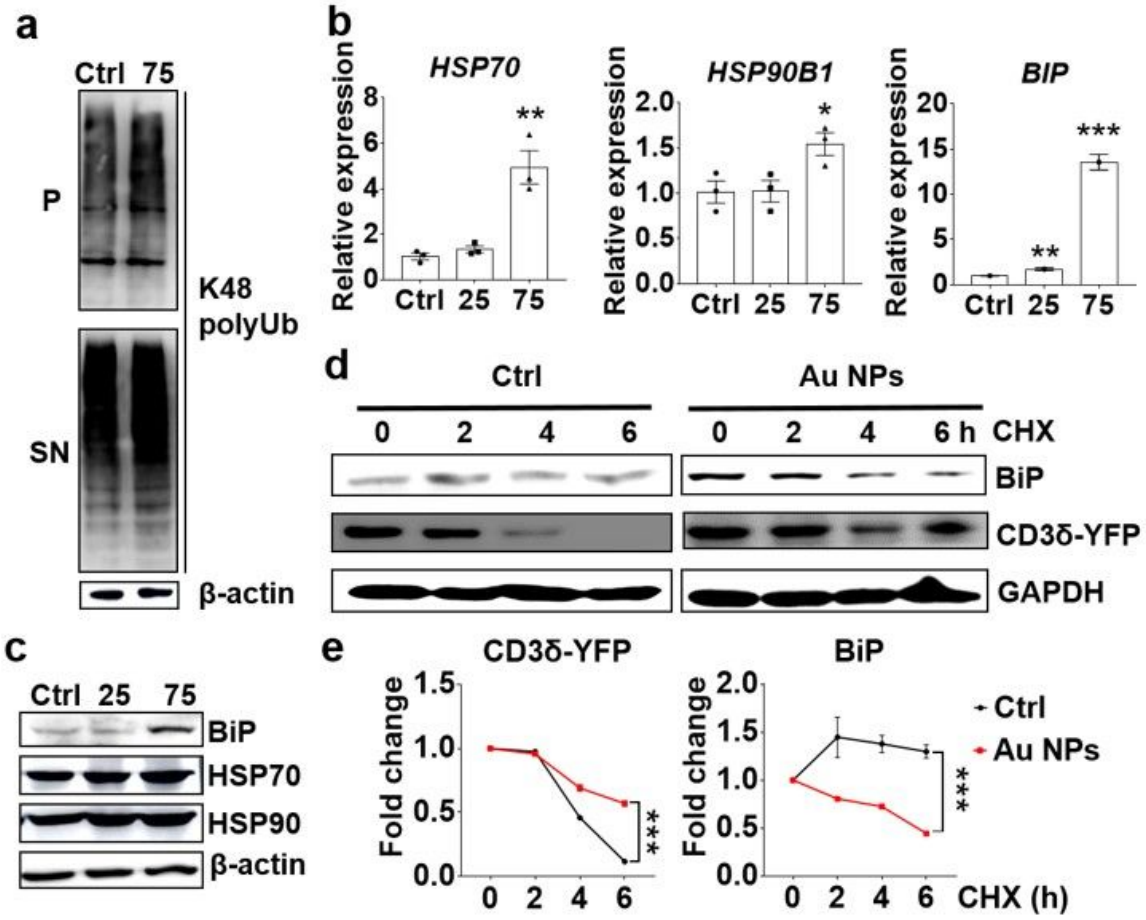

Figure 3

Au NPs induce the accumulation of misfolded/unfolded proteins and interfere with the ERAD process. a-c Cells were exposed to medium alone (Ctrl) or containing Au NPs (25 and 75 μg/ml) for 24 h. a Western blot analysis on the misfolded/unfolded protein marker of K48 polyUb. β-actin was used as loading control. P, pellet; SN, supernatant. b mRNA expression of the PQC related gene of HSP70, HSP90B1 and BIP. c Western blot analysis of the PQC related proteins of HSP70, HSP90 and BiP. β-actin was used as loading control. d-e Degradation rate of CD3-δ-YFP and BiP in control cells (Ctrl) and cells treated with Au NPs for 24 h. Cells were treated with cycloheximide (CHX, 50 μg/ml) to block protein synthesis for 2, 4 or 6 h before protein levels were examined by Western blot. d Representative Western blot results of CD3-δ-YFP and BiP. GAPDH was used as loading control. e Time-dependent protein degradation rate of CD3-δ-YFP and BiP. Data in b and e are presented as the mean ± SEM of three experiments. *, $p<0.05$; **, $p<0.01$; ***, $p<0.001$ vs. control.

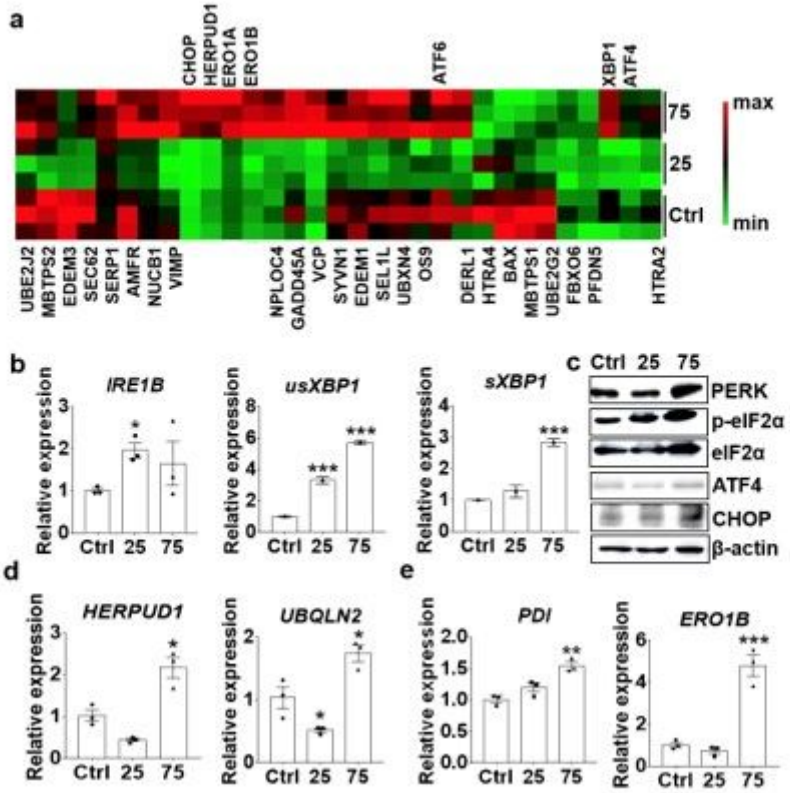

Figure 4

Au NPs affect UPR effects and ER stress. Cells were treated with medium alone (Ctrl) or Au NPs (25 and 75 μg/ml) for 24 h. a Heatmap of the transcriptional profiling of ER-associated genes. The genes indicated above the heatmap have been studied further. b mRNA expression of UPR related IRE1B, usXBP1, sXBP1. c Western blot analysis of the UPR related proteins of PERK, phospho-eIF2α, eIF2α, ATF4 and CHOP. β-actin was used as loading control. d mRNA expression of ERAD-related genes HERPUD1 and UBQLN2. e mRNA expression of ER stress-related genes of PDI and ERO1B. Data in b, d and e are presented as mean ± SEM of three experiments. *, $p<0.05$, **, $p<0.01$, ***, $p<0.001$ vs. control.

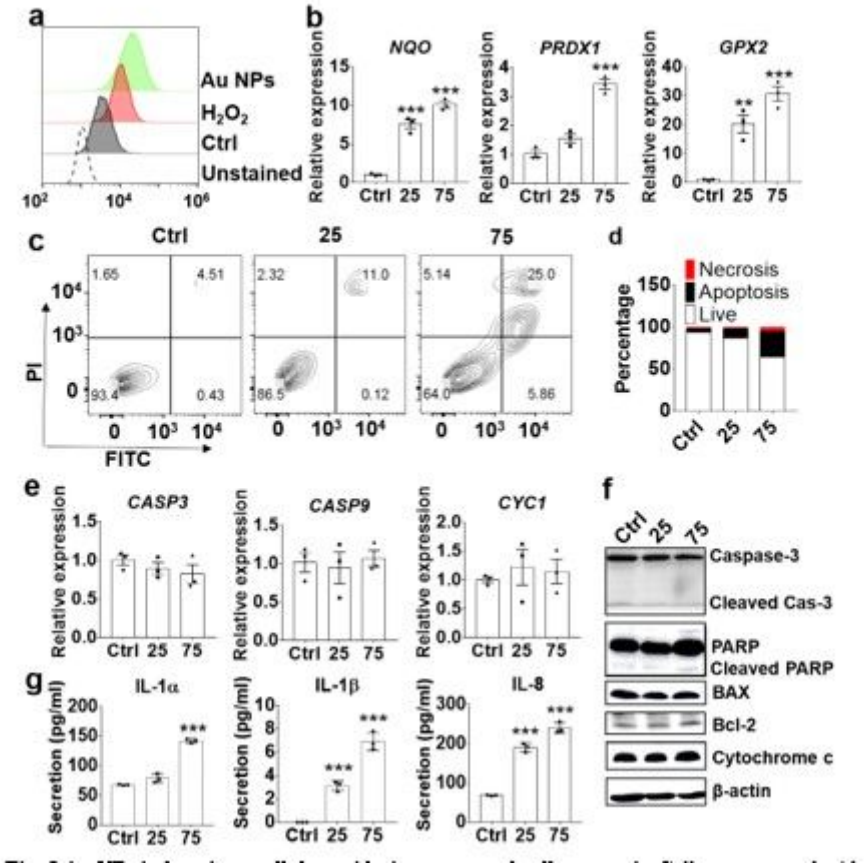

Figure 5

Au NPs induce intracellular oxidative stress and cell apoptosis. Cells were treated with medium alone (Ctrl) or Au NPs (25 and 75 μg/ml) for 24 h. a The intracellular ROS levels were evaluated by flow cytometry after DCFDA staining. H2O2 served as positive control. b mRNA expression of oxidative stress-related genes NQO, PRDX1 and GPX2. c Cell apoptosis that evaluated by flow cytometry. Live: FITC-/PI-; early apoptosis: FITC+/PI-; late apoptosis and post-apoptotic necrosis: FITC+/PI+; necrosis: FITC-/PI+. d Quantitative data of the flow cytometric analysis of cell apoptosis. e mRNA expression of mitochondrial apoptotic related-genes encoding caspase-3 (CASP3), caspase-9 (CASP9) and cytochrome c (CYC1). f Western blot analysis of the mitochondrial apoptosis-related proteins caspase-3, PARP, BAX, Bcl-2 and cytochrome c. β-actin was used as loading control. g Secreted levels of IL-1α, IL-1β and IL-8, evaluated by ELISA. **, $p<0.01$, ***, $p<0.001$ vs. control.

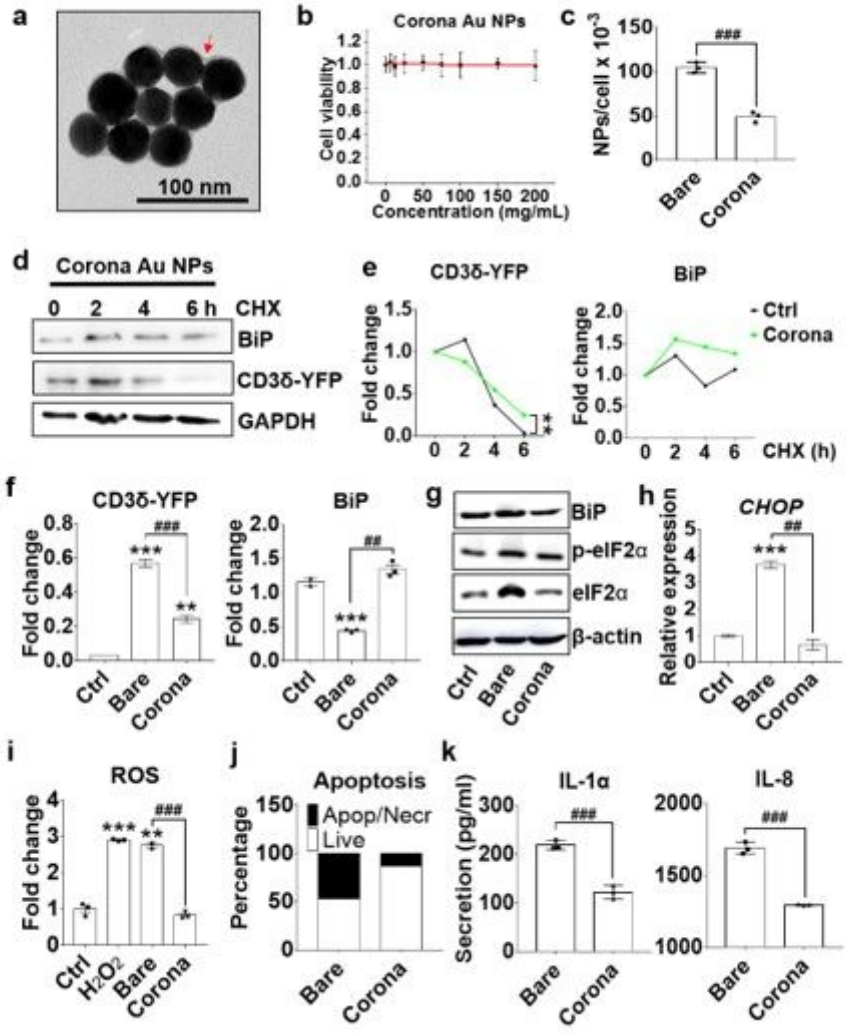

Figure 6

The protein corona mitigates the Au NPs effects on the intracellular protein quality control system. a TEM image depicting the protein corona on Au NPs (red arrow). b Viability of cells exposed to corona Au NPs. c Quantitative evaluation of intracellular Au NPs assessed by ICP-MS. d-f Degradation rate of CD3-δ-YFP and BiP in control cells (Ctrl) and corona Au NP-treated cells for 24 h. Cycloheximide (CHX, 50 μg/ml) was used to block protein synthesis for 2, 4 or 6 h before protein levels were examined by Western blot. d Representative Western blot of CD3-δ-YFP and BiP. GAPDH was used as loading control. e Time-dependent protein degradation rate of CD3-δ-YFP and BiP. f Quantitative analysis of the degradation rate of CD3-δ-YFP and BiP measured after 6 h of CHX treatment. Data are expressed as fold change vs. cells not treated with CHX. g-k Cells were treated for 24 h with medium alone (Ctrl) or Au NPs (75 μg/ml) either bare or with a protein corona. g Western blot analysis of the PQC-related proteins BiP, phospho-eIF2α and eIF2α. β-actin was used as loading control. h mRNA expression of the ER stress-related gene CHOP. i Intracellular ROS levels evaluated by flow cytometry. H2O2 served as positive control. j Quantitative evaluation of the flow cytometric analysis of cell apoptosis. k Secreted levels of IL-1α and IL-8, evaluated

by ELISA. Data in E and F are presented as the mean ± SEM of three independent experiments. Data in c and h-k are presented as mean ± SEM of triplicate samples. **, p<0.01, ***, p<0.001, vs. control. ##, p<0.01, ###, p<0.001 vs. bare.

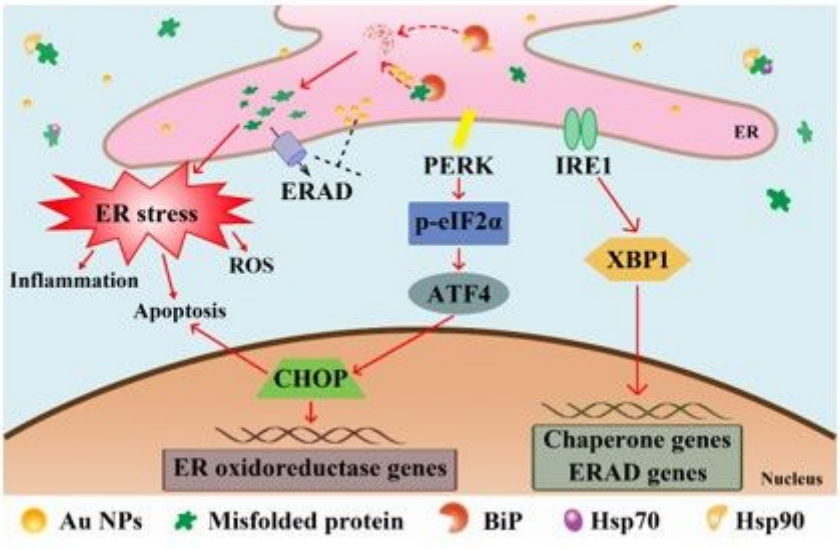

Figure 7

The proposed model of NP-induced PQC dysfunction. Au NPs interfere with PQC functions in the ER, leading to the accumulation of misfolded/unfolded proteins thereby triggering ER stress. The Au NP-induced accumulation of misfolded/unfolded proteins in the ER and ERAD dysfunction lead to ER stress that activates the PERK-p-eIF2α-ATF4-CHOP pathway. This will ultimately trigger intracellular ROS accumulation, cell apoptosis and inflammatory responses. Conversely, the activated UPR pathway of IRE1-XBP1 upregulates the expression of chaperone and other ERAD-associated factors to restore the ER stress.

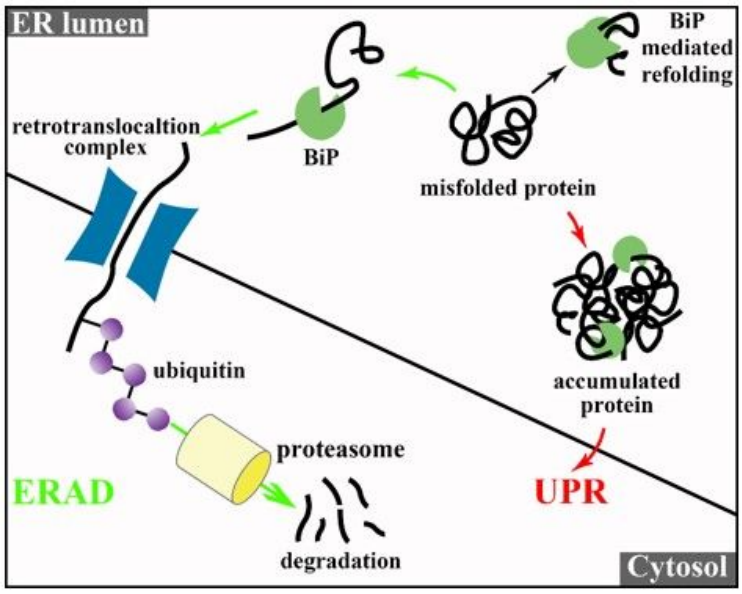

Figure 8

Schema 1. The ER related protein quality control process in cells.

Supplementary Files

This is a list of supplementary files associated with this preprint. Click to download.

- SupportingXXInformationPQC0926yang.docx